

Structure–activity relationships in linear oligoester ion-channels†

Thomas Murray Fyles* and Horace Luong

Received 23rd September 2008, Accepted 10th November 2008

First published as an Advance Article on the web 17th December 2008

DOI: 10.1039/b816649h

The ion transport activity of eighteen linear oligoesters was assessed using a quantitative fluorescence assay to monitor the collapse of a pH gradient across a vesicle bilayer membrane. Significant activity was associated with compounds that have extended lengths comparable to the thickness of the bilayer membrane, and with the most hydrophilic members of the compounds surveyed. Substantial differences in activity between constitutional isomers were also observed. The aggregation of active compounds in aqueous solution was detected by a pyrene fluorescence probe, and subsequently detected as a rate-limiting step in a sequential vesicle experiment.

Introduction

The accompanying paper describes the solid-phase synthesis of a suite of structurally related linear oligoesters.¹ The focus of this paper is to survey the activity of this set of compounds with a view to uncovering mechanistic information. At the same time, we are interested to explore the general problem of assessing the relative membrane activity of a large number of compounds.

A variety of techniques have been exploited to assess the transport activity of synthetic channel-forming compounds.² Although conductance experiments in planar bilayers offer the least ambiguous method for determining the formation of discrete channels, they are very poorly suited for a survey. Each experiment is time-consuming and the control of concentration of an active compound in the membrane is hit-and-miss. Although we have in fact done a survey using this technique,³ and have explored techniques to introduce compounds reliably,⁴ the problems with the method are largely unresolved on a reproducible and quantitative level.

Vesicle techniques offer more scope for structure–activity surveys, and there are many examples of this type of investigation.^{5–7} Even so, vesicle techniques are subject to artefacts as the hoped-for channel activity is often indistinguishable from the detergent-like lysis of the vesicles.² Since vesicle batches are a finite and variable resource, most surveys will require multiple batches with the inherent batch-to-batch variation as a confounding factor in the analysis of the survey results. Every additional control experiment designed to detect artefacts and assist in batch-to-batch normalization adds to the overhead of the survey and decreases the throughput.

Ratiometric fluorescence techniques, in which a dye is entrapped in the vesicle during preparation and thereafter reports the ionic concentration environment through a ratio of two emission intensities, are potentially valuable in this context. A common technique uses hydroxypyrene trisulfonate (HPTS) to report the

internal pH of a vesicle population.^{2,8} The emission maximum for HPTS is about 510 nm in both the acid and conjugate base forms. However, the excitation wavelength of the acidic form (403 nm) is significantly different from that of the conjugate base form (460 nm) so that the acid/base ratio is directly reflected in the emission intensity modulation produced by alternating excitation at the two wavelengths. In essence, the modulated emission signal can report the effective pH within the vesicle. The use of a ratio of emission intensities, rather than absolute emission intensity at a single wavelength, reduces batch-to-batch variability simply due to different scattering from different population distributions of the vesicles. Even with these advantages, the assay has typically only used for quantitative comparisons within a single batch of vesicles.^{2,8}

We report here a methodology based on the HPTS assay that can be used to generate quantitative data for the survey of the activity of a library of compounds. We employ the method to explore structure–activity relationships within the set of oligoester ion-channel compounds prepared,¹ and as a consequence derive a model for the way in which these compounds act in bilayer membranes.

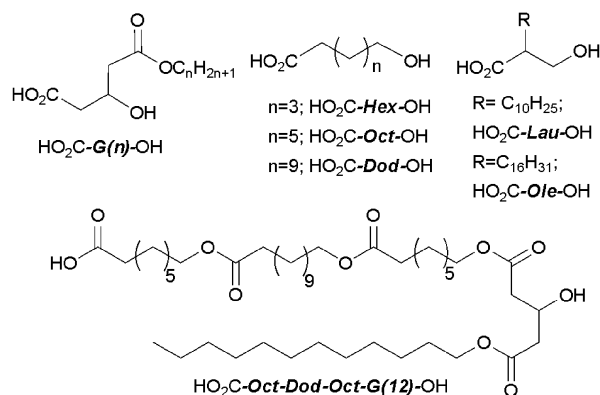
Results and discussion

Compounds surveyed

The solid-phase synthesis of the compounds for this study is described in an accompanying paper.¹ The method used works from a set of hydroxyacid building blocks to produce linear trimeric, tetrameric, and pentameric oligoesters (Scheme 1). Three types of building blocks were used: monoalkyl esters of hydroxyglutaric acid (HO₂C-*G*(*n*)-OH), ω-hydroxy alkanolic acids (e.g. HO₂C-*Oct*-OH), and α-hydroxymethyl alkanolic acids (e.g. HO₂C-*Lau*-OH). The compounds can be named using a sequence of the components in the same fashion as oligopeptide structures are specified; unlike peptide names we specify the carboxyl and hydroxyl termini for clarity. Thus HO₂C-*Oct-Dod-Oct-G*(12)-OH is a tetramer consisting of the ω-hydroxyacids containing eight, twelve, and eight carbons terminated with the dodecyl ester of the glutaric acid unit.

Department of Chemistry, University of Victoria, PO Box 3066, Victoria, BC, Canada V8W 3V6. E-mail: tmf@uvic.ca; Fax: +1 250 721 7147; Tel: +1 250 721 7150

† This paper is dedicated to Prof. Seiji Shinkai in recognition of his many contributions to supramolecular chemistry.



Scheme 1 Building blocks and naming system for compounds.

Vesicle assay

The vesicles for the HPTS assay were prepared, sized, and purified as reported previously from a 8:1:1 mixture of phosphatidyl choline, phosphatidic acid and cholesterol (PC:PA:Ch).⁹ The preparation method routinely gave vesicle populations with an average diameter of 340 ± 50 nm and an average lipid concentration of 0.43 ± 0.05 mM in 10 mM phosphate buffer at pH 6.4. The assay involved injection of a transporter in methanol solution, a short (30–60 s) period of baseline data collection, followed by injection of a NaOH pulse to establish a pH gradient for proton efflux. Data collection for a period of 500–800 s was followed by addition of detergent to establish the final emission intensity for the experiment. Methanol alone produces a slow leakage that was determined at various times within each set of experiments.

The data consists of emission intensity at 510 nm modulated by alternating excitation at 403 nm and 460 nm on a 2 + 2 s cycle. The concentration of the conjugate base form is related to the emission intensity at 510 nm during the period when the dye is excited at 460 nm (E_{460}) while the concentration of the protonated form is related to the emission intensity at 510 nm during the period when the dye is excited at 403 nm (E_{403}). A plot of $\log(E_{403}/E_{460})$ versus pH for HPTS in homogenous solutions is linear and yields an intercept pK_a (7.25; lit.¹⁰ 7.3) and a slope factor which allows the internal pH (pH_{in}) of the vesicle to be calculated from the data as a function of time with a time resolution of 4 s (Fig. 1). Following detergent lysis, the dye reports the external pH, typically 7.8, assumed to be a constant throughout the experimental period due to the relatively small encapsulation volume.

The collapse of the pH gradient *via* channels will give “all or nothing” behaviour resulting in an apparent first-order process since the signal will depend only on the decreasing number of vesicles that retain the gradient.⁵ Thus a plot of $\ln([H^+]_{in} - [H^+]_{\infty}) / ([H^+]_0 - [H^+]_{\infty})$ versus time should be linear and give an apparent first-order rate constant for the experiment. The expected linearity is generally observed for data acquired after an initial period of 100 s following the pH pulse. This biphasic behaviour has been discussed previously.¹¹ The initial fast step is due to adjustment to osmotic and ionic imbalance stresses on the vesicles that allows random formation of pores with concomitant pH equilibration. This is followed by a solution-diffusion stage in which ion exchange processes control the gradient collapse. It is the second step which we wish to accelerate *via* added transporter,

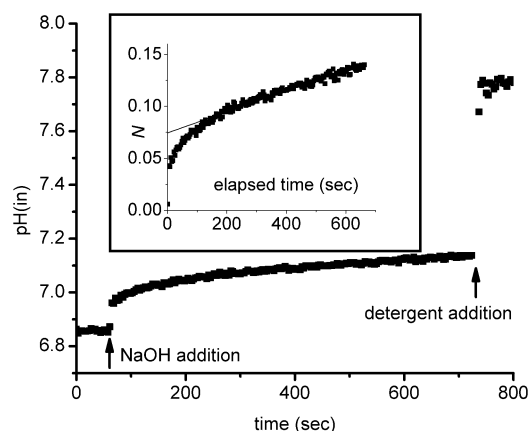


Fig. 1 Internal vesicle pH as a function of time as derived from HPTS emission data (PC:PA:Ch 0.42 mM; 10 mM phosphate buffer; 5.6 μ M HO₂C-Oct-Dod-Oct-G(12)-OH). Inset: N as a function of time following NaOH addition plus linear fit to data >100 s.

so in the data analysis we omitted the first 100 s of data following the base pulse.

Although the process described above (intensity converted to pH and then to proton concentrations) can be used to generate rate data,¹² we note that this sequence involves an antilogarithmic step followed by a logarithmic step embedded in an otherwise linear set of relationships between observed emission intensities and a rate constant. This suggests that the conversion to pH can be avoided. However, the first-order function relates the observed change to a specific gradient represented by the difference between initial and final values which is unique to each experiment. This is a type of normalization that is essential for comparisons between different experiments. Any process to avoid conversion to pH must also contain this type of normalization. Accordingly, we defined a normalized extent of transport (N) defined below, where the subscripts 0, ∞ , and t denote the emission ratios before the base pulse, after detergent lysis, and at some intermediate time respectively. In essence N gives the extent of transport between 0 and 100%.

$$N = \frac{\left(\frac{E_{403}}{E_{460}} \right)_t - \left(\frac{E_{403}}{E_{460}} \right)_0}{\left(\frac{E_{403}}{E_{460}} \right)_\infty - \left(\frac{E_{403}}{E_{460}} \right)_0}$$

For small extents of transport where the pH gradient is very close to constant, a plot of N versus time is linear between 100 and 800 s following the base pulse; an apparent rate constant can be derived from the slope (inset to Fig. 1). The result of the process is equivalent to converting to pH and is simpler to implement. All data presented is derived from this “direct” method.

A survey conducted over several batches of vesicles including many different transporters with activities ranging from significant to negligible requires a comparison of observed rates that is independent of batch-to-batch variations in the vesicles or in other experimental parameters such as mixing. Moreover, the quality of the assay data depends upon the addition of an optimum concentration of transporter so the rates are significantly above

background methanol leakage rate yet still within the linearization constraints discussed above. Even with well-controlled protocols, replicates conducted from a single batch of vesicles under optimal concentrations varied by a factor of $\pm 20\%$. Thus the direct normalization of rates *via* a ratio based on the repeated observation of a standard compound will give rise to significant scatter.

Our approach to this survey problem rests on the routine observation of a linear relationship between the observed rate constant (k_{obs}) and the transporter concentration ($[\text{Tr}]$), observed with a single batch of vesicles.⁹ In addition, the intercept of the linear relationship is typically equal (within experimental error) to the directly determined methanol leakage rate for the batch of vesicles (k_{MeOH}). Thus: $k_{\text{obs}} = m[\text{Tr}] + k_{\text{MeOH}}$. This relationship allows the slope parameter (m) to be determined from experiments for a series of concentrations in transporter that can be selected to meet the constraints of the assay and the activity of the compound. Within the range of the established linear relationship, a rate at a defined concentration can be interpolated, and it is this rate that can be compared across a series of compounds to assess relative activity.

Operationally, each compound was assessed in a preliminary fashion to establish an appropriate concentration range. If significant activity was found, the compound was then reassessed in a focussed way at two or three different concentrations in the acceptable range. Some compounds showed insignificant activity relative the background rate; k_{MeOH} shows batch-to-batch variation but took an average value of $(2.4 \pm 1.1) \times 10^{-4} \text{ s}^{-1}$ over a 15 month period. "Significant" activity was assessed as at least twice the background leakage rate for the particular batch of vesicles at a transporter concentration between 15 and 30 μM . A particularly "leaky" batch of vesicles will therefore mask the activity of a moderately active compound.

When the dataset was complete, the overlapping experimental concentration ranges were inspected to establish a reference concentration that would permit interpolation for the majority of active compounds. In the event, this was chosen to be 32 μM . The rate constant at this concentration ($k_{32\mu\text{M}}$) was then calculated from m and k_{MeOH} . The activity of each compound was then interpolated at this concentration using the experimentally observed values of m and k_{MeOH} . The data is summarized in Table 1.

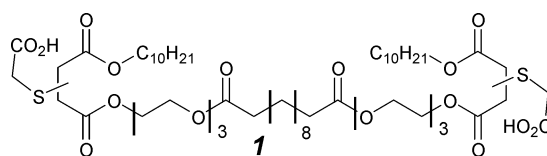
Structural influences on transport rate

A quick inspection of the data in Table 1 indicates that the variation in activity across the series of compounds is very modest. This is partly a result of the fairly close structural similarities between the compounds, is also an indication that the building blocks utilized have some deficiencies. This point is established by considering the activity of the "grandparent" compound **1** (entry 19); this compound is more than twice as active as the most active of the set of linear oligoesters. Compound **1** has approximately the same extended length as $\text{HO}_2\text{C-Oct-Dod-Oct-G(12)-OH}$ and approximately the same number of methylenes. However **1** contains two triethylene glycol segments and two carboxylic acid groups. Both factors would increase the hydrophilicity of **1** relative to $\text{HO}_2\text{C-Oct-Dod-Oct-G(12)-OH}$.

Table 1 Transport rate constants determined^a

| Compound | Range (μM) | $k_{32\mu\text{M}}$ ($\text{s}^{-1} \times 10^4$) | |
|----------|--|---|---------------|
| 1 | $\text{HO}_2\text{C-Oct-Dod-Oct-G(10)-OH}$ | 17–49 | 6.3 ± 2.1 |
| 2 | $\text{HO}_2\text{C-Oct-Dod-Oct-G(12)-OH}$ | 8.4–53 | 6.1 ± 1.7 |
| 3 | $\text{HO}_2\text{C-Oct-Dod-Oct-G(14)-OH}$ | 28 | 3.0 |
| 4 | $\text{HO}_2\text{C-Oct-Dod-Oct-G(16)-OH}$ | 14–46 | 3.9 ± 1.4 |
| 5 | $\text{HO}_2\text{C-G(12)-Oct-Dod-Oct-OH}$ | 15–49 | 2.6 ± 0.2 |
| 6 | $\text{HO}_2\text{C-Oct-Oct-Dod-G(12)-OH}$ | 25–41 | 3.1 ± 0.5 |
| 7 | $\text{HO}_2\text{C-Dod-Oct-Oct-G(12)-OH}$ | 19–49 | 3.6 ± 0.3 |
| 8 | $\text{HO}_2\text{C-Dod-Dod-Oct-G(12)-OH}$ | 49 | ^c |
| 9 | $\text{HO}_2\text{C-Oct-Dod-Dod-G(12)-OH}$ | 56 | ^c |
| 10 | $\text{HO}_2\text{C-Oct-Oct-Oct-G(12)-OH}$ | 42 | ^c |
| 11 | $\text{HO}_2\text{C-Dod-Dod-Dod-G(12)-OH}$ | 31 | ^c |
| 12 | $\text{HO}_2\text{C-Hex-Oct-Hex-Oct-G(12)-OH}$ | 16–41 | 6.7 ± 4.1 |
| 13 | $\text{HO}_2\text{C-Lau-Oct-Dod-Oct-G(12)-OH}$ | 18–44 | 4.1 ± 1.7 |
| 14 | $\text{HO}_2\text{C-Ole-Oct-Dod-Oct-OH}$ | 17–44 | 3.9 ± 0.1 |
| 15 | $\text{HO}_2\text{C-Oct-Dod-Oct-Lau-OH}$ | 19–37 | 7.6 ± 2.2 |
| 16 | $\text{HO}_2\text{C-Oct-Dod-Oct-Oleate}^b$ | 27–32 | ^c |
| 17 | $\text{HO}_2\text{C-Oct-Dod-Oct-OH}$ | 26 | ^c |
| 18 | $\text{HO}_2\text{C-Oct-Dod-OH}$ | 39 | ^c |
| 19 | 1 | 9–32 | 16 ± 6 |

^a HPTS assay and data treatments as described in the text. ^b Compound terminates as the oleate ester; no terminal hydroxyl group. ^c Activity insignificantly different from background at the given concentration.



On the other hand, the relatively small range of activities indicates that the solid-phase methodology reliably produces the compounds indicated. We previously reported that dimers and trimers such as $\text{HO}_2\text{C-Oct-G(12)-OH}$ and $\text{HO}_2\text{C-Oct-Dod-G(12)-OH}$ are active detergents in vesicles.⁹ This type of impurity was not detected in the synthetic work¹ but it is reassuring that the compounds are clearly free of this type of active short sequence impurity. The types of impurities detected in the synthesis are of the type represented as entries 17 and 18 in Table 1; this type of dimer/trimer is very inactive. As a consequence the impurities from the synthesis play little role in the observed transport activities.

The suite of compounds contains a number of sets of constitutional isomers (entries 2, 5, 6, and 7; 8 and 9). Within these groups, some members are significantly more active than others. The most significant difference uncovered is between the $\text{HO}_2\text{C-Oct-Dod-Oct-G(12)-OH}$ and $\text{HO}_2\text{C-G(12)-Oct-Dod-Oct-OH}$ pair (entries 2 and 5). This difference in activity are consistent with a preferred orientation for insertion into the vesicle, among other possibilities. Also significant is the marked lack of activity of compounds which are longer and shorter than $\text{HO}_2\text{C-Oct-Dod-Oct-G(12)-OH}$ (entries 8–11 compared to 2, 5–7). The implication of this result is that there must be a match between the overall length of the compound and the thickness of the bilayer membrane. One plausible rationale would focus on a membrane-spanning orientation of the most active compounds that was inaccessible or energetically unfavoured for shorter or longer structures. The number of esters appears to be relatively unimportant for the one example contained in the suite of compounds (entries 2 and 12).

The series of compounds HO₂C-*Oct-Dod-Oct-G(n)*-OH (entries 1–4) shows a significant reduction in activity as the lipophilicity of the compound increases with increasing alkyl chain length. The partition of a monomer to a membrane would be expected to increase in the opposite direction, indicating that another factor must influence the activity more profoundly. A similar inverse relationship with lipophilicity is noted in the *Lau* and *Ole* comparisons (entries 14–16); of these the oleate terminated compound HO₂C-*Oct-Dod-Oct-Oleate* is both the least hydrophilic and the least active. These results point to the adverse effect on activity of the hydrophobic character of the compounds. One rationale suggests a competing aggregation might occur for the most lipophilic compounds.

Aggregation in aqueous solution

The fluorescence spectrum of pyrene is a sensitive probe of local solvent polarity and has been used to determine the critical micelle concentration (cmc) of conventional surfactants.¹³ The ratio of the intensities of the first and third vibronic bands of the pyrene emission (I_1/I_3) shifts from ~1.5 in aqueous solution to ~1 for pyrene bound in a low-polarity micellar aggregate. Fig. 2 shows the evolution of I_1/I_3 for an aqueous pyrene solution as a function of the concentration of HO₂C-*Oct-Dod-Oct-G(16)*-OH. From the raw data alone it is clear that the compound provides a predominantly non-polar environment for the pyrene at concentrations that lie in the range of the transport experiments discussed above. The experimental data fit to a logistic function to yield a concentration for the half-maximum change (16 μ M for the data of Fig. 2). Entirely equivalent curves were obtained for the other HO₂C-*Oct-Dod-Oct-G(n)*-OH compounds with half-maximal concentration points in 12–20 μ M range.

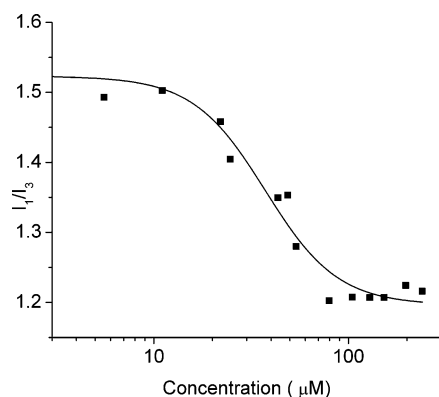


Fig. 2 Ratio of vibronic band intensities (I_1/I_3) for fluorescence of pyrene as a function of HO₂C-*Oct-Dod-Oct-G(n)*-OH concentration (10 mM phosphate buffer, 75 mM Na₂SO₄, pH 6.4, [pyrene] = 2.3 μ M).

It is not correct to view this half-maximal concentration as the cmc for the compound since the transition from “free” to “bound” occurs over a wide concentration range; in a true micelle-forming solution the transition is typically very abrupt and occurs at ~mM concentration where the surfactant monomer concentration greatly exceeds the pyrene concentration (>10⁴:1). At 10 μ M in HO₂C-*Oct-Dod-Oct-G(16)*-OH, there is only a 30-fold excess of compound relative to pyrene. Even if discrete micelles of very low aggregation number (*e.g.* <100) did form, the number of these

micelles would be insufficient to bind all the available pyrene. Alternatively, the aggregation of the compound could be non-specific such that the nature of the aggregate evolves in the 10–100 μ M concentration range to produce the poorly defined transition reflected in the data.

Migration of compound between vesicles

Whatever the origin of the broad transition observed in Fig. 2, it is evident that all HO₂C-*Oct-Dod-Oct-G(n)*-OH compounds form appreciable aggregates in the concentration range of the transport experiments. Given the structural similarities in the suite of compounds, this conclusion probably applies to the entire set of oligoesters. In the transport experiment a stock solution in methanol is injected into the aqueous vesicle solution. It is likely that aggregates will form very rapidly as the methanol disperses into solution. In order for transport to be observed, the compound, either as a monomer at an equilibrium concentration, or as the entire aggregate, must migrate to, and insert into, a vesicle. The pyrene experiments described above suggest that aggregates form at very low concentration, thus the free monomer concentration must also be very low, and therefore give rise to a slow process of insertion into vesicles. Direct aggregate insertion is also likely to be a slow process due to slow diffusion and steric and hydration repulsion forces between the partners.¹⁴

We have previously explored this type of migration issue with a sequential experiment in which a batch of vesicles is readied for a transport experiment and then divided into two samples.⁵ Transport is initiated by transporter addition to one of the samples of vesicles and allowed to proceed for a period of time. A second sample of “fresh” vesicles is then added and the transport is again monitored. If the added transporter is fully able to migrate between vesicles and any aggregated state, the rate following the addition of the fresh vesicles should be the same as in the initial period since all that has changed is the size of the population of vesicles that the transporter can access. Conversely, any inhibition due to slow partitioning will result in the second rate being significantly slower than the first rate. An example of this type of experiment is illustrated in Fig. 3 for an experiment involving methanol (lower curve) and HO₂C-*Oct-Dod-Oct-G(16)*-OH (upper curve). The sharp step on vesicle addition reflects the lower pH of the new

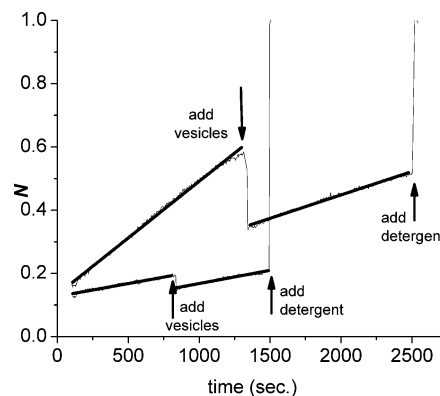


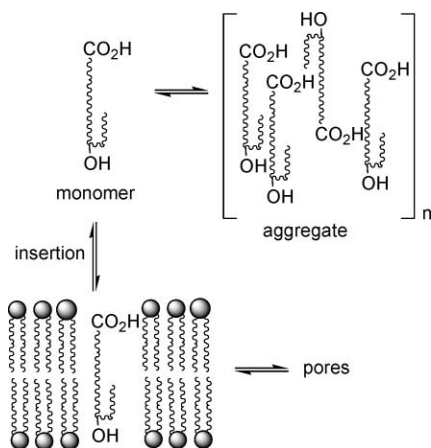
Fig. 3 Fractional transport as a function of time for sequential addition of vesicles. Lower trace: methanol; upper trace HO₂C-*Oct-Dod-Oct-G(n)*-OH (44 μ M in final solution). Heavy line indicates linear fit.

sample of vesicles; there is no osmotic stress response since this stage has already occurred in the second vesicle batch.

The ratio of the second rate to the first rate for the methanol leakage is 1.0 (within experimental error) as expected for a simple partitioning of a water-soluble solute. The corresponding rate ratio for HO₂C-*Oct-Dod-Oct-G(16)*-OH is 0.4 ± 0.1 indicating substantial inhibition of migration to the second batch of vesicles. The corresponding values for the alkyl homologs *~G(12)*, and *~G(14)* are 0.7 ± 0.2 , and 0.4 ± 0.1 respectively. All three values are less than one indicating that a slow partition step plays a role in determining transport activity. The least lipophilic dodecyl derivative does show a higher rate ratio than the tetradecyl or hexadecyl derivatives. This is suggestive of the formation of an aggregate that controls the rate through the concentration of the available monomer. Although transport by HO₂C-*Oct-Dod-Oct-G(10)*-OH initiated by pH jump is clearly first order, when initiated by transporter addition the transport shows a sigmoidal relationship of *N* with time during the first part of the experiment. This inhibits a rate ratio determination, but also indicates a complicated partitioning behaviour.

Conclusions

Taken together, the data presented above suggest the sequence of events illustrated in Scheme 2 occurring during the transport experiment. The initial injection of a methanolic solution of the transporter rapidly produces an aggregate of the compound or micellar solution which controls the monomer concentration at a low level. The pyrene experimental results suggest that the monomer concentration is below 10 μM after the aggregate forms. The compound then partitions, *via* the monomer, to the vesicles. The transport results from constitutional isomers are consistent with some preferred orientation of insertion into the vesicle bilayer membrane, but this is neither conclusively demonstrated nor essential to the following discussion. The transport results suggest that at least some of the inserted monomers adopt a transmembrane orientation, thereby resulting in the length dependence noted in the data. Finally the inserted monomers combine to stabilize and aqueous pore for the transport of ionic species.



Scheme 2 Mechanistic proposal for transport.

Within this working proposal, there are several areas that require clarification and which suggest the direction of future exploration. The formation of transmembrane pores would be expected to give rise to discrete open-close behaviour in a planar bilayer conductance experiment. A preliminary investigation observed this expected behaviour for HO₂C-*Oct-Dod-Oct-G(12)*-OH and HO₂C-*G(12)-Oct-Dod-Oct-OH*:¹² a more thorough examination will be reported separately.

A more critical issue relates to the overall low activity of these compounds. The implication of the pathways in Scheme 2 is that higher monomer concentrations would yield more active transporters. Since monomer concentration is proposed to be controlled by the aggregate, it is clear that the library of compounds must include derivatives that are substantially more hydrophilic than the components explored to date. This can readily be achieved *via* more hydrophilic building blocks; oligo ethyleneglycol ethers in place of hydrocarbon chains is one possible direction to explore. The solid-phase methodology is compatible with coupling to amino acids using a Fmoc protocol and this would be a source of hydrophilic components to expand the set of building blocks.¹²

The principle goal of this and the accompanying paper has been achieved in that the creation and exploration of the activity of library of compounds has been thoroughly explored. The weaknesses in the synthesis approach were discussed.¹ Apart from the low activity of the compounds, the main difficulty in conducting a vesicle-based assay is the control of batch-to-batch variability. The procedures described in this report will reliably and quantitatively compare the activities of different compounds over a range of activities, and a period of time. However, the conclusions that can be drawn from the data are directly limited by the procedures to reproducibly control the vesicles on which the assay is based.

Experimental

Vesicle preparation

The general procedure for vesicle preparation and the HPTS fluorescence assay has been described elsewhere.⁹ A chloroform solution containing PC:PA:cholesterol (8:1:1 mole ratio) was dried *in vacuo*. The approximately 60 mg lipid film was hydrated with 1 mL of internal buffer solution (9.9 μM HPTS, 10.1 mM Na₃PO₄, 74.7 mM Na₂SO₄, pH adjusted to 6.4 using H₃PO₄) and transferred into a small test tube. The suspension was frozen with liquid nitrogen and then thawed at room temperature over ten minutes. This cycle was repeated three times. The mixture was then equilibrated in an ice bath and sonicated with a 13 mm tip probe (Heat Systems) for 20 seconds with 2 second pulses (at 50% duty cycle and 20% power output) followed by a 30 second delay time; this cycle was repeated until a total sonication time of two minutes was reached. The liposomes were then allowed to anneal overnight. The vesicle solution was then sized 19 times through a 400 nm polycarbonate Nucleopore filter using a LiposoFast membrane extrusion apparatus (Avestin) and purified using an external buffer solution (10.1 mM Na₃PO₄, 74.7 mM Na₂SO₄, pH adjusted to 6.4 using H₃PO₄) equilibrated PD-10 Sephadex G-25 column. The first three cloudy drops were discarded but thereafter the cloudy fraction was collected and diluted to 5.00 mL using the external buffer solution. A typical preparation contained 340 nm diameter

vesicles (dynamic light scattering) and a lipid concentration of typically 7 mg/mL as determined by the Barlett assay.¹⁵ The vesicle solution was used within 24 hours of preparation.

HPTS ion transport assay

In a fluorimetric cell was added a magnetic stir bar, 2.00 mL of the external buffer solution, 100 μ L of the stock vesicle solution and 30 μ L of a 0–4.3 mM MeOH solution of the oligoester compound. HPTS emission was monitored at 510 nm and excitation wavelengths of 403 and 460 nm were used concurrently. Raman emission artifacts were not significant based on the examination of fluorescence spectra of vesicles made without the HPTS dye. After a 30 second equilibration time, 50 μ L of 0.5 M NaOH was added (time = zero) through an injector port. After about 500 seconds, the vesicles were lysed with a 50 μ L 5% Triton[®] X-100 solution. The data was imported into a Microsoft Excel worksheet and all data prior to 100 seconds from the introduction of NaOH was ignored. The relative intensity of $E_{403\text{nm}}/E_{460\text{nm}}$ (F) was calculated. The adjusted mean time was determined from the difference of the actual time and about 60–100 seconds (t_0) after the NaOH injection. The extent of transport was calculated using $(F_i - F_0)/(F_i - F_0)$; F is the relative emission intensity at time i , F_0 is the relative emission intensity at t_0 , F_i is the relative emission intensity when vesicles are lysed. The extent of transport is plotted against time and the slope of the resulting line was the rate constant for the particular concentration tested. The error in rate assessed from duplicates was $\pm 20\%$ within one batch of vesicles.

Compound aggregation studies

Pyrene was purified by column chromatography through a silica gel column and using cyclohexane as the eluent. The purity of the pyrene was established using lifetime measurements, where a mono-exponential decay for aqueous solutions is obtained for pure samples. In a low-volume fluorescence cell various volumes of the ion channel solution (mM in concentrations) in methanol (1–30 μ L) were injected and methanol was added so that the total volume of methanol was 30 μ L. A 5 μ L aliquot of a methanolic pyrene solution (0.025 mg/mL) was injected and 0.3 mL external buffer. The solution was vigorously shaken

and followed by a three min delay before measurements were taken. The measurements were recorded at 20.0 ± 0.1 °C with an excitation of 331 nm (slit width of 3 nm) and emission spectra were collected between 365–400 nm (slit width of 1 nm). The spectra were collected with a background subtraction of a solution containing all components excluding pyrene. The method of determining the 1 and 3 band ratio is reported in the literature.¹⁶

Acknowledgements

The assistance of Prof. Cornelia Bohne and Ms. Effie Li with the fluorescence experiments is gratefully acknowledged. This work was supported by NSERC-Canada.

References

- 1 T. M. Fyles and H. Luong, *Org. Biomol. Chem.*, 2008.
- 2 S. Matile and N. Sakai, in *Analytical Methods in Supramolecular Chemistry*, ed. C. A. Schalley, Wiley-VCH, Weinheim, 2007, pp. 381–418.
- 3 T. M. Fyles, R. Knoy, K. Müllen and M. Sieffert, *Langmuir*, 2001, **17**, 6669–6674.
- 4 M. B. Buchmann, T. M. Fyles and T. Sutherland, *Bioorg. Med. Chem.*, 2004, **12**, 1315–1324.
- 5 T. M. Fyles, T. D. James and K. C. Kaye, *J. Am. Chem. Soc.*, 1993, **115**, 12315–12321.
- 6 G. W. Gokel, R. Ferdani, J. Liu, R. Pajewski, H. Shabany and P. Uetrecht, *Chem. Eur. J.*, 2001, **7**, 33–39.
- 7 M. E. Weber, P. H. Schlesinger and G. W. Gokel, *J. Am. Chem. Soc.*, 2005, **127**, 636–642.
- 8 V. Siderov, F. W. Kotch, G. Abdrakhmanova, R. Mizani, J. C. Fettinger and J. T. Davis, *J. Am. Chem. Soc.*, 2002, **124**, 2267–2278.
- 9 T. M. Fyles, C. Hu and H. Luong, *J. Org. Chem.*, 2006, **71**, 8545–8551.
- 10 R. P. Haugland and M. T. Z. Spence, *The Handbook. A Guide to Fluorescent Probes and Labelling Technologies*, Molecular Probes, Eugene, OR, 2005.
- 11 C. L. Kuyper, J. S. Kuo, S. A. Mutch and D. T. Chiu, *J. Am. Chem. Soc.*, 2007, **128**, 3233–3240.
- 12 H. Luong, University of Victoria, 2008.
- 13 K. Kalyanasundaram and J. A. Thomas, *J. Am. Chem. Soc.*, 1977, **99**, 2039–2044.
- 14 J. Israelachvili, *Intermolecular and Surface Forces*, 2nd edn, Academic Press, London, 1992.
- 15 R. R. C. New, in *Liposomes: a practical approach*, ed. R. R. C. New, IRL Press, Oxford, 1990.
- 16 Y. Chang, M. Kellermann, M. Becherer, A. Hirsch and C. Bohne, *Photochemical & Photobiological Sciences*, 2007, **6**, 525–531.